PCCP

Accepted Manuscript

This is an *Accepted Manuscript*, which has been through the Royal Society of Chemistry peer review process and has been accepted for publication.

Accepted Manuscripts are published online shortly after acceptance, before technical editing, formatting and proof reading. Using this free service, authors can make their results available to the community, in citable form, before we publish the edited article. We will replace this *Accepted Manuscript* with the edited and formatted *Advance Article* as soon as it is available.

You can find more information about *Accepted Manuscripts* in the Information for Authors.

Please note that technical editing may introduce minor changes to the text and/or graphics, which may alter content. The journal's standard Terms & Conditions and the Ethical guidelines still apply. In no event shall the Royal Society of Chemistry be held responsible for any errors or omissions in this *Accepted Manuscript* or any consequences arising from the use of any information it contains.

Journal Name

ARTICLE

Distinct and Dramatic Water Dissociation on GaP(111) tracked by Near-Ambient Pressure X-ray Photoelectron Spectroscopy

Xueqiang Zhang[a,b] and Sylwia Ptasinska[a,c]*

Water adsorption and dissociation on a GaP(111) crystal surface are investigated using Near-Ambient Pressure X-ray Photoelectron Spectroscopy (NAP XPS) in a wide range of pressures ($\sim10^{-10}$-5 mbar) and temperatures ($\sim$300-773 K). Dynamic changes in chemical evolution at the H_2O/GaP(111) interface are reflected in Ga $2p_{3/2}$, O 1s, and P 2p spectra. In the pressure-dependent study performed at room temperature, an enhancement of surface Ga hydroxylation and oxidation with an increase in H_2O pressure is observed. In the temperature-dependent study performed at elevated pressures, two distinct regions can be defined in which drastic changes occur in the surface chemistry. Below 673 K, the surface Ga hydroxylation and oxidation progress continuously. However, above 673 K, a large-scale conversion of surface O–Ga–OH species into non-stoichiometric Ga hydroxide along with oxidation of surface P atoms occurs through an intermediate state. The NAP XPS technique enabled us to experimentally track the chemistry at the H_2O/GaP interface under near-realistic conditions, thereby providing evidence to compare with recent theoretical efforts to improve the understanding of water-splitting mechanisms and photo-corrosion on semiconductor surfaces.

Introduction

Semiconductor-based photo-electro-chemical (PEC) solar cells are capable of converting solar energy into hydrogen via water-splitting reactions, thereby supplying environmentally benign and sustainable energy.[1-6] Such devices are of particular interest, because solar energy can be converted to chemical energy and stored in the form of hydrogen, a promising candidate for sustainable and clean fuels in the future.[7-13] Due to the limited availability of information on atomic and electronic structures of a semiconductor surface under realistic conditions, a comprehensive picture of molecular chemistry at the water/electrode interface is not yet been available.[14-16] In addition, factors such as the corrosion of electrodes or complications with appropriate matching of a semiconductor band gap to a typical solar spectrum make the practical implementation of PEC devices challenging.[14-16] In contemporary technology, the most efficient PEC devices comprise III-V semiconductor photoelectrodes,[17-23] which are typically phosphide-based.[9, 24] Although tremendous progress

has been made with regard to interface passivation and dielectric properties of III-V semiconductors, the fabrication of an ideal dielectric/semiconductor interface remains a challenge due to the lack of a complete understanding of chemistry at the interface of such systems. Since PEC processes occur in an aqueous environment, it is essential to understand the nature of water interactions with semiconductors and the possible oxidation and reduction mechanisms at the H_2O/semiconductor interface.[4, 6]

Hydrogen-networking and hydrogen transfer are the fundamental processes to be addressed in order to understand and characterize semiconductor surfaces that are exposed to a water environment.[25, 26] Therefore, much effort has been made to explore hydrogen-bond networks at the water/semiconductor interface. For instance, Wood et al. performed *ab initio* molecular dynamic simulations that revealed an increase in water hydrogen-bond strength on a Ga/InP(100) surface that facilitates water dissociation and local proton hopping.[4, 15] Using first-principles density functional theory (DFT)

calculations, Munoz-Garcia et al. reported the presence of hydride-like H atoms on the GaP(110) surface as a result of water dissociation via hydrogen-bonded intermediates.[27] There are also other experimental[14, 28-31] and theoretical[6, 16, 26, 32] studies on the role of hydrogen bonds in water interactions with III-V semiconductor surfaces such as GaP,[6, 14] GaAs,[28, 31] GaSb,[26, 32] and InP.[16, 29, 30] These studies clearly emphasize the importance of such local hydrogen-bonding in the interfacial dynamics and chemistry of semiconductors.

Moreover, several studies have also focused on the role of other surface species, such as oxides, hydroxyls, and adsorbed water molecules.[4, 15, 16, 27] Water, in its molecular form, and water dissociation products can greatly influence the chemical and electrical structures of semiconductor surfaces. It has been suggested that there is a correlation between water splitting and the existence of surface oxygen species on III-V semiconductor electrode surfaces.[4, 7, 14, 18] In a recent investigation of water adsorption onto a GaP(100) surface under ultra-high vacuum (UHV) conditions,[14] it was observed that water can be either molecularly or dissociatively adsorbed, according to reflection anisotropy spectroscopy. However, in the same work, no changes in the chemistry of surface Ga or P atoms were observed by UHV X-ray photoelectron spectroscopy (XPS) performed after exposure of the GaP(100) surface to water.[14] A recent theoretical study showed that the effects of water behavior on GaP(110) depend strongly on water coverage.[27] These results indicated an enhancement in water dissociation at higher coverage. Therefore, to obtain a deeper insight into water interactions with semiconductors, it is necessary to conduct an *in situ* study of the H_2O/semiconductor interfacial chemistry under more realistic conditions.[15]

The present study was motivated by the lack of experimental data on chemical characterizations of H_2O/semiconductor interfaces such as H_2O/GaP,[14, 27] particularly at near-ambient conditions. As reported previously, it is possible for a molecular environment to induce a difference between the surface chemistry at near-ambient conditions and the surface chemistry occurring under UHV conditions.[33, 34] To achieve an understanding of the H_2O/semiconductor interface at the atomic level, our work reports the results of an NAP XPS study of H_2O interactions with the GaP(111) surface. The NAP XPS is capable of tracking the chemical evolution at such interfaces under near-realistic conditions. Our results can significantly contribute to understanding and improving the technological applications of GaP, an electrode material that is incorporated into many current PEC devices[3, 5, 35] and is considered to be one of the most promising photocathode materials for water and CO_2 reduction.[4, 6, 8, 27]

Experimental Section

All *in situ* photoelectron spectra were recorded using a SPECS near-ambient pressure X-ray photoelectron spectrometer equipped with an Al Kα X-ray tube coupled to a Micro-FOCUS 600 X-ray monochromator, a preparation chamber with an ion gun for surface cleaning, a reaction cell (filled with a gas up to a pressure of 20 mbar) mounted to an analyzer chamber, and a PHOIBOS 150 hemispherical energy analyzer (HEA) with a

differentially pumped electrostatic lens system. A detailed description of the present experimental set-up and procedure can be found in our previous work.[28, 31] The binding energy (BE) scale for photoelectron spectra was calibrated using the P $2p_{3/2}$ peak, which corresponds to the P–Ga bond with a BE of 128.8 eV.[36, 37] All spectra were corrected for the background of scattered photoelectrons using Shirley's method and were fitted with a multiple Gaussian/Lorentzian peak combination using SpecsLab2 and CasaXPS software. This hybrid function was selected because the Lorentzian function represents physical effects (i.e., intrinsic lifetime broadening of the core-level hole state), whereas the Gaussian function represents the contribution of instrumental effects (e.g., the response function of the electron analyzer, the profile of the X-ray line shape, phonon broadening, or surface charging). We allowed a flexibility of 0.15 eV for the BE and full width at half-maximum (FWHM) for all fitted peaks.

The undoped (n-type semiconductor, resistivity of ~0.3 Ωcm) simple planar GaP crystalline surface with (111) orientation was purchased from Sigma-Aldrich, USA. High-purity silver paint (from Supplies SPI, USA) was used to increase conductivity, and the sample was thoroughly degassed before it was introduced into the system. The GaP(111) crystal was gently cleaned by Ar^+ bombardment in the preparation chamber. Since the ion bombardment method can induce surface modifications, we systematically examined the GaP surface as a function of the Ar^+ energy and exposure time. The Ar^+ beam (0.4 keV, 45° with respect to the sample surface, 10 min, and 2 cycles) at a pressure of 3×10^{-6} mbar successfully removed the native oxide layer and other contaminants. Then, the sample was annealed to 725 K for surface structure restoration.[38-40] The BE of the Ga $2p_{3/2}$ peak maximum for the Ga-P bonds is located at 1117.3 eV, while a small shoulder at BE of 1116.8 eV is expected to appear in the event of a metallic phase formation (Ga-Ga bonds). The purity and electronic structure of the surface were monitored by taking photoelectron spectra after each cycle. Neither contamination nor Ga-Ga bond formation were observed after the above mentioned treatment. Survey photoelectron spectra of GaP(111) samples before and after Ar^+ bombardment are displayed in Fig. S1 in Supplementary Information (SI). After cleaning and before H_2O introduction, the GaP(111) sample was transported, contamination-free, from the preparation chamber to the directly connected analysis chamber with the reaction cell (a base pressure of 5×10^{-10} mbar). The crystal temperature was read by a K-type (chromel-alumel) thermocouple sandwiched between the crystal and the molybdenum sample holder. The photoelectron spectra were obtained by heating the sample at 5 K/min (heating rate) followed by 20 min of stabilization. Typically, the average time of photoelectron spectrum recording was about one hour. Prolonged heating in an H_2O environment can induce minor changes (~5%) in the intensity of photoelectron peaks, particularly at higher temperatures. There were no differences in the type of formed species between the plotted data and the data obtained after prolonged heating at temperatures below 673 K. The ultra-pure water was

degassed via multiple freeze–pump–thaw cycles prior to use.

Pressure dependence: To compare the pressure-dependent
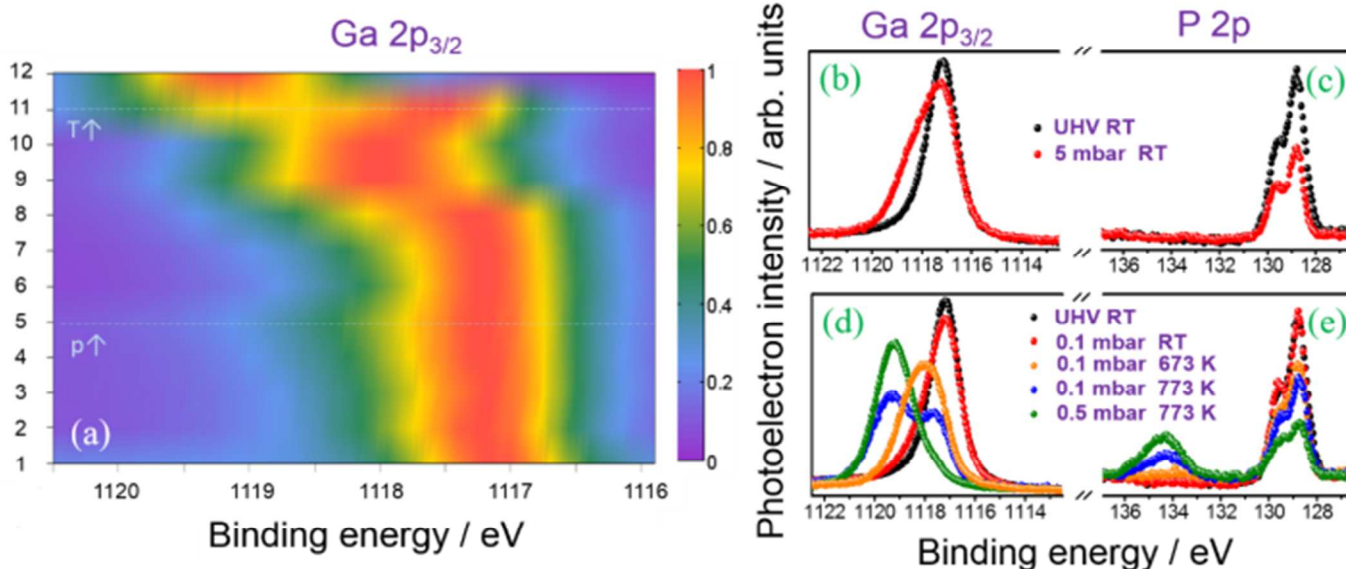
Fig. 1 (a) Contour plot of the Ga 2p$_{3/2}$ signal under various conditions (y-axis): UHV, 0.005, 0.05, 0.5, and 5 mbar of H$_2$O at RT (1-5); 273, 373, 473, 573, 673, and 773 K at the H$_2$O pressure of 0.1 mbar (6-11), and 773 K at an H$_2$O pressure of 0.5 mbar (12). The obtained contour plot was recorded intermittently after each increase of pressure or temperature followed by condition stabilization. The signal at each specific condition was collected within one hour; (b) and (c) Comparison of high resolution Ga 2p$_{3/2}$ and P 2p spectra obtained under UHV (5×10^{-10} mbar) conditions and at the H$_2$O pressure of 5 mbar and RT (~300 K). Due to the short mean free path of photoelectrons from Ga 2p$_{3/2}$ and P 2p, the signal intensity decreases significantly at the pressure of 5 mbar. Therefore, the Ga 2p$_{3/2}$ spectra are normalized to unit intensity of main peaks and shifted to the same background lines; (d) and (e) Comparison of high resolution Ga 2p$_{3/2}$ and P 2p spectra obtained under UHV (5×10^{-10} mbar) and under 0.1 mbar at RT, 673 K and 773 K, and under 0.5 mbar at 773 K.

The C 1s spectra were frequently recorded throughout the entire experimental procedure to monitor possible C-based contaminants introduced by water or by the silver paint. However, no contamination was observed within our detection limit.

Two types of *in situ* XPS experiments were performed on the GaP(111) crystal surface; in these experiments, the crystal was exposed to different i) H$_2$O pressures and ii) temperatures. For a comprehensive comparison, most of the recorded photoelectron spectra taken under these different conditions are displayed in the SI. The pressure-dependent study was implemented in the H$_2$O pressure range of UHV (5×10^{-10} mbar) to 5 mbar at room temperature (RT, ~300 K). Photoelectron spectra were taken at UHV, 0.005 mbar, 0.05 mbar, 0.5 mbar, and 5 mbar in the reaction cell. The evolution of *in situ* photoelectron spectra for Ga and P elements corresponding to these pressures are presented in Fig. S2. The temperature-dependent study was conducted in the temperature range from RT to 773 K under a constant H$_2$O pressure environment (0.1 mbar or 0.5 mbar). The evolutions of *in situ* photoelectron spectra under an H$_2$O pressure of 0.1 mbar or 0.5 mbar for different temperatures are displayed in Fig. S3. Because the surface chemistry may be influenced by H$_2$O exposure durations, time-dependent photoelectron spectra have also been recorded under extreme conditions and are presented in Figs. 4 and S4.

Results

chemical changes that occur due to H$_2$O interactions with the GaP(111) surface, photoelectron spectra for Ga 2p$_{3/2}$ and P 2p, shown in Fig. 1, were taken at RT under two extreme pressure conditions: under UHV and at an H$_2$O pressure of 5 mbar. The Ga 2p$_{3/2}$ features are broader and shifted toward higher BEs at 5 mbar when compared with the UHV spectra, while only slightly noticeable effects of broadening and displacement are observed for the P 2p features. Due to photoelectron scattering with gas-phase molecules, a shorter photoelectron inelastic mean free path (IMFPs) at higher pressures causes a decrease in signal intensity, the photoelectron spectra for the Ga 2p$_{3/2}$ and P 2p were normalized to unit intensity of the main peaks, which is a peak with the highest intensity, and shifted to the same background lines (Fig. 1).

A detailed analysis of pressure-dependent evolutions for Ga 2p$_{3/2}$ and O 1s spectra reveals complementary changes (Fig. 2). The Ga 2p3/2 spectra are fitted with three components at binding energies (BEs) of 1117.3 ± 0.05 eV (peak A), 1118.1 ± 0.1 eV (peak B) and 1119.2 ± 0.15 eV (peak C), corresponding to Ga–P bonds, O–Ga–OH and O$_x$–Ga–(OH)$_{3-x}$ (0≤x≤1) species on the surface, respectively (Fig. 2a). These BEs in peak assignments are consistent with BE values obtained from earlier extensive XPS studies on Ga-based semiconductor materials (crystals and standard oxide samples) under UHV conditions.[36, 41-44] However, the two latter structures (i.e., O–Ga–OH and O$_x$–Ga–(OH)$_{3-x}$), instead of forming pure phase, represent non-stoichiometric compounds; this will be discussed in detail subsequently. The UHV Ga 2p$_{3/2}$ consists of one peak (A), while the presence of two higher BE peaks (B and C) is due to

dissociative water adsorption onto the GaP(111) surface. The increasing photoelectron intensity of peaks B and C correlates with increasing H_2O pressures (Fig. 2a).
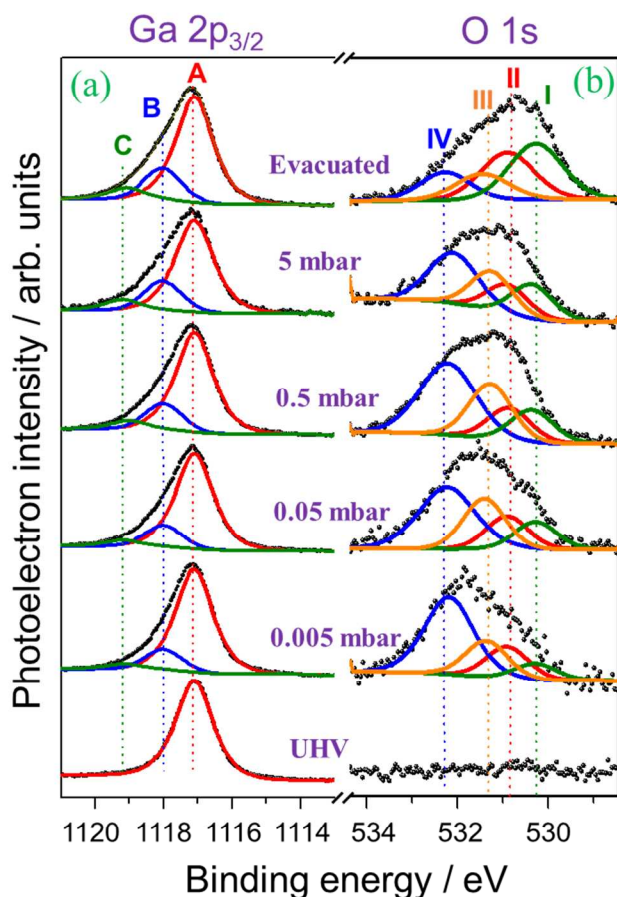
Fig. 2 Evolution of high-resolution Ga $2p_{3/2}$ and O 1s spectra of the GaP(111) surface at various H_2O pressures at RT and after H_2O is pumped away ("Evacuated"). (a) Peak assignments of Ga $2p_{3/2}$ spectra: A - Ga–P bond, B - O–Ga–OH, and C - O_x–Ga–$(OH)_{3-x}$; (b) Peak assignments of O 1s spectra: I - Ga–O–Ga , II - Ga–OH, III - H2O---HO–Ga, and IV - molecularly adsorbed H_2O. The symbols "---"and "–" are used to indicate the molecular interaction and the covalent bond, respectively. To better visualize the changes, the photoelectron intensity axis is rescaled.

The O 1s spectra are fitted with four components at BEs of 530.6 ± 0.1 eV (peak I), 531.2 ± 0.1 eV (peak II), 531.7 ± 0.1 eV (peak III), and 532.6 ± 0.2 eV (peak IV), corresponding to Ga–O–Ga, Ga–OH, OH species attached to H_2O molecules via hydrogen bonds (H_2O---HO–Ga), and molecularly adsorbed H_2O, respectively (Fig. 2b). In the case of Ga–OH (peak II), the hydroxyl group can bridge another surface atom (M–O(H)–M, where M = Ga, and also M = P in the case of the temperature-dependent study described below) or can exist as a terminal group (atop OH, M–OH, where M only represents Ga). The photoelectron peak assignments of different O-based

components are also consistent with previous *in situ* XPS studies on H_2O adsorption and dissociation on metal surfaces,[33, 45, 46] and Ga-based surface compounds.[28, 31] The broad peak at 532.6 ± 0.2 eV (peak IV) is attributed to intact H_2O molecules. There are three possibilities of the H_2O molecule's existence in an intact form on the surface: 1) when H_2O is directly adsorbed via two lone-electron pairs that are bonded as Lewis base to an empty hybrid p-orbital of Ga;[4, 6, 15, 27] 2) when H_2O is hydrogen bonded to surface OH groups;[24, 35, 36] or 3) when H_2O is bonded to other H_2O molecules,[47, 48] as components of the hydrogen-bond network in the latter two cases. These three forms of adsorbed water molecules can contribute to a broader structure for peak IV because they have relatively close BEs that are mainly influenced by hydrogen bonding. The peak area ratio of IV and III components is estimated to be between 2:1 and 3:1 depending on the H_2O pressure, and the ratio decreases to 1:1 after H_2O is pumped away. A similar behavior was observed in studies on H_2O interactions with Cu(110) performed using *in situ* XPS.[45] The peak area ratio of the dissociative products (peaks I-III) and intact water molecules (peak IV) is approximately 6:1 upon evacuation (Fig. 2b, "Evacuated"), which suggests the presence of a higher dissociation yield of H_2O molecules resulting in oxidation and hydroxylation of the GaP(111) crystal surface.

It is worth noting that the shape evolution seen in the O1s spectra under different pressure conditions reflects changes observed in the Ga $2p_{3/2}$ spectra (Fig. 2). No noticeable changes were observed for Ga $2p_{3/2}$ (Fig. S4) and other elemental spectra (not shown) collected for four hours at an H_2O pressure of 5 mbar. This time-dependent study indicates that prolonged water exposure at an H_2O pressure of 5 mbar and at RT does not induce observable changes in the surface chemistry.

Temperature dependence: To compare the temperature-dependent chemical changes due to H_2O interactions with the GaP(111) surface at elevated temperatures, photoelectron spectra for Ga $2p_{3/2}$ and P 2p were taken under UHV (RT), H_2O pressure of 0.1 mbar (RT, 673 and 773 K), and 0.5 mbar and 773K, as shown in Fig. 1d and 1e.

A detailed analysis of temperature-dependent evolution for Ga $2p_{3/2}$ and O 1s spectra reveals complementary changes (Fig. 3). For all photoelectron spectra, we can clearly identify two temperature regions in which distinctive interfacial chemistry occurs at the regions below and above 673 K (Fig. S3). The Ga $2p_{3/2}$ and O 1s spectra are fitted and assigned in a similar manner as for the pressure-dependent study, with the exception of an additional peak formation above 673 K (Fig. 3).

The Ga $2p_{3/2}$ spectra are fitted with four components at BEs of 1117.3 ± 0.05 eV (peak A), 1118.1 ± 0.1 eV (peak B), 1119.2 ± 0.15 eV (peak C) and an additional peak at 1117.6 ± 0.1 eV (peak D), corresponding to Ga–P bonds, O–Ga–OH, O_x–Ga–$(OH)_{3-x}$ species, and Ga oxides (hereinafter referred to as Ga_2O-like species, since the BE maximum for this peak matches the BE value for stoichiometric Ga_2O[42, 44, 49, 50]), respectively (Fig. 3a). Apart from peak A, all the other peaks result from H_2O adsorption and its dissociation on the GaP(111) surface. The peak assignments are based on previous XPS studies related to

Ga-based materials.[28, 31, 42, 44, 49, 50] As mentioned above, these assignments do not suggest that the species are stoichiometric compounds in their pure phase. Their structure can contain the Ga–P bond involving stabilizing surface P and its oxides, which can only deplete or evaporate at much higher temperatures.
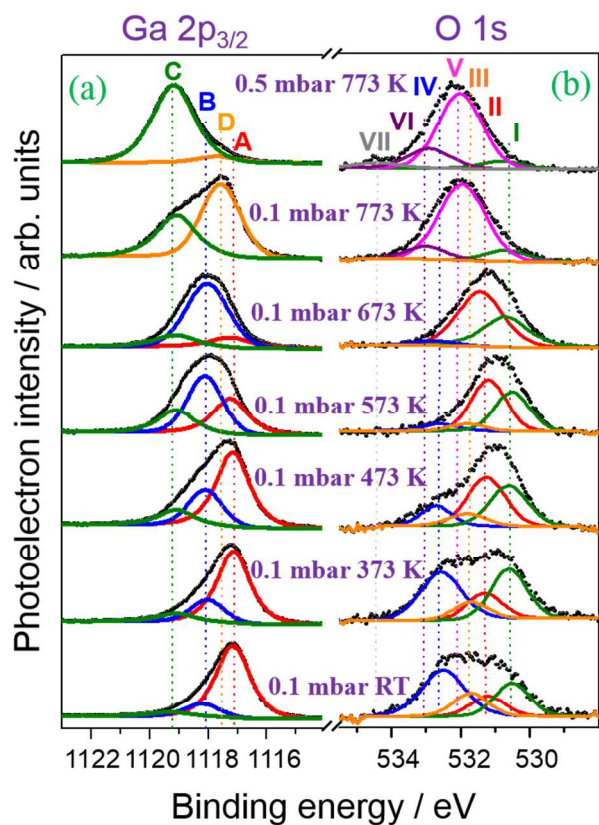
Fig. 3 Evolution of high-resolution Ga $2p_{3/2}$ and O 1s spectra of the GaP(111) surface at different temperatures in an 0.1 mbar/0.5 mbar H_2O environment. (a) Peak assignments of Ga $2p_{3/2}$ spectra: A - Ga–P bonds, B - O–Ga–OH, and C - O_x–Ga–$(OH)_{3-x}$, and D - Ga_2O-like species; (b) Peak assignments of O 1s spectra: I - Ga–O–Ga, II - Ga–OH, III - H_2O---HO–Ga, IV - molecularly adsorbed H_2O, V - Ga$(OH)_3$, VI – P oxides, VII - P_2O_5-like species. To better visualize the changes, the photoelectron intensity axis is rescaled.

In the lower temperature region (below 673 K), the Ga (both $2p_{3/2}$ and 3d) peaks are largely broadened, and their maxima shift toward higher BEs with an increase in temperature compared to relatively minor changes in the P 2p spectra (Fig. 1e and S3). The observed shift of the Ga $2p_{3/2}$ peak maximum is mainly due to a greatly enhanced intensity of peak B assigned to O–Ga–OH. In the higher temperature region (above 673 K), peak C at a BE of 1119.2 ± 0.15 eV develops with a greatly increased intensity, along with the appearance of peak D at a BE of 1117.6 ± 0.1eV. Simultaneously, peaks A and B are almost completely quenched. The same trend is also observed in Ga 3d spectra, as shown in Fig. S3b, which indicates that the chemical changes are not restricted only to a few top atomic layers but rather expand to deeper layers. However, as assessed from the time-dependent results (Fig. 4), the newly formed

component D is not stable, and its intensity gradually decreases as the intensity of peak C increases.

At 773 K, the Ga $2p_{3/2}$ spectrum consists mainly of one component, which is peak C at the H_2O pressure of 0.5 mbar (Fig. 3a). This drastic change in the Ga $2p_{3/2}$ spectra at both elevated pressures and elevated temperatures is well represented by the contour plot in Fig. 1a. The Ga $2p_{3/2}$ peak representing pure Ga–P bonds shifts from its original position (1117.3 eV) to higher BEs upon increasing H_2O pressures. Moreover, this shift is coupled with peak broadening. Below 673 K, the O–Ga–OH species are the main H_2O dissociation products, but above this temperature the Ga $2p_{3/2}$ spectrum splits into two maxima, thereby representing a mixed phase of oxide and hydroxide species; finally, at elevated pressures and temperatures, the surface is in the chemical state largely corresponding to Ga hydroxides. Additionally, Figs. 1d and S3c show a comparison of P 2p spectra indicating the formation of P-based oxides (P–O) at a BE of 134 eV above 673 K.[51-53]
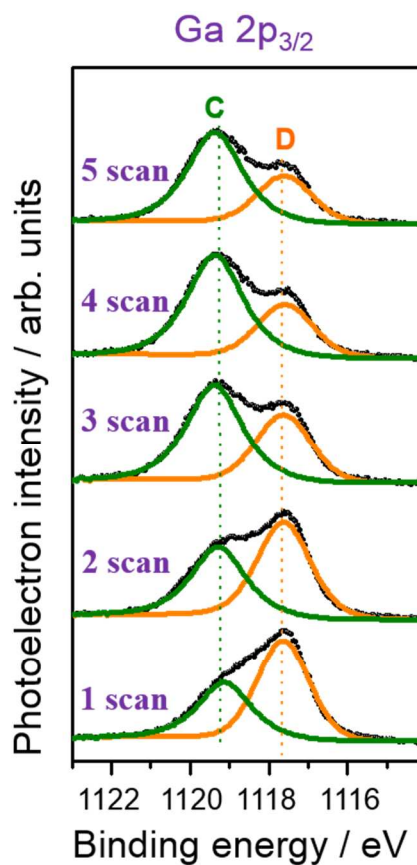
Fig. 4 Time-dependent Ga $2p_{3/2}$ spectra obtained for the GaP(111) surface at a temperature of 773 K and an H_2O pressure of 0.1 mbar, which were continuously taken within 4 hours. Peak assignments: C-O_x–Ga–$(OH)_{3-x}$, and D -Ga_2O-like species.

In the case of the O 1s spectra (Fig. 3), the peak assignments for the low-temperature region are the same as those for peaks I-IV in the O 1s spectra at elevated pressures in Fig. 2. However, the two lower BE components that are assigned to Ga–O–Ga (peak I) and Ga–OH (peak II) surface species exhibit significantly enhanced intensities at elevated temperatures (Fig. 3). Simultaneously, the two higher BE peaks, which correspond

to OH bonded to H_2O (peak III, H_2O---HO–Ga) and molecularly adsorbed H_2O (peaks IV), exhibit strong quenching. The relative signal intensity (peak area) ratio for these two peaks remains at 1:1 up to 673 K, after which both peaks vanish. A similar temperature behavior was reported in previous *in situ* XPS studies involving H_2O dissociation on GaAs[28, 31] and metal[33, 45, 46] surfaces at near-ambient pressures. For the high temperature region shown in Fig. 3b, the formation of other O-based species is observed at a BE of 532 eV (peak V). This peak is attributed to the $Ga(OH)_3$ structure.[42] Two minor contributions at BEs of 534.3 eV (peak VII) and 533 eV (peak VI) are also observed and can be assigned to P oxides.[53-55]

Discussion

Molecularly adsorbed water: The present pressure- and temperature-dependent studies allow us to determine the evolution of chemistry at the H_2O/GaP interface under near-ambient conditions. Initially, the interacting water molecule that possesses two lone-electron pairs can bind as a Lewis base to an empty hybrid p-orbital of Ga-rich surfaces.[4, 6, 15, 27] However, according to DFT calculations by Jeon et al.,[6] such an adsorption structure at low (~ sub-monolayer) coverage is relatively unstable, with the adsorption energy calculated to be 0.41 eV. Therefore, water molecules are expected to desorb at a relatively low temperature (i.e., 209 K). Low-temperature desorption was also observed for molecularly-adsorbed and fully or partially hydrogen-bonded H_2O released from the GaAs(110) surface below RT in a temperature-programmed desorption study.[56] Additionally, a previous XPS study on water interactions with GaP(100) at RT under UHV conditions reported a partially solvated GaP surface, particularly at RT, with an estimated coverage of 0.25 ± 0.2 monolayer.[14] However, the adsorption energy increases with higher surface H_2O coverage.[27] In our study, the GaP(111) surface is exposed to elevated H_2O pressures (up to 5 mbar); thus, much higher water coverage is expected in comparison to conditions in UHV studies. A higher coverage can be verified by higher intensities of peaks attributed to H_2O molecules adsorbed on the GaP surface in the O 1s spectra in Figs. 2b and 3b. As seen in these figures, peak IV exhibits a particularly broad structure with a maximum in the range of 532.5-532.8 eV, which suggests water cluster formation. Typically, a water monomer is not frequently observed even at low temperatures.[57] At elevated pressures, water diffusion on a surface facilitates clustering of neighboring water molecules and formation of hydrogen bonds.[58] Recent DFT calculations have suggested that two H_2O molecules can interact with each other via hydrogen bonds, forming a bridge between surface Ga and P atoms (Ga---OH_2---OH_2---P).[27] Such a bridge enables the proton transfer process between H_2O and the P atom, because water molecules are bonded via hydrogen interactions that weaken their O–H bonds, thereby leading to the formation of a Ga–OH---OH_2---H–P structure.[27]

Water dissociation: It has been reported that the calculated energy barriers for water dissociation on various materials are lower for clusters or packed monolayers of water compared to a monomeric water molecule.[45, 59, 60] For example, Munoz-Garcia et al. reported a relatively low dissociation barrier of 40 meV on a fully solvated GaP(110) surface (with a coverage ≥ 4 monolayers), which is only slightly higher than the thermal energy at RT (26 meV).[27] The authors explained that at higher H_2O coverage (in our case higher H_2O coverage is correlated to higher H_2O pressure), local hydrogen-bond networks can be formed, and such an instantaneous solvent environment leads to shorter intermolecular water distances that are necessary for proton transfer.[4, 15] A similar concept was reported by Tatarkhanov et al. regarding two possible competing interactions: between H_2O and a metal surface and between H_2O molecules.[60] A low coverage facilitates the former case and leads to the formation of H_2O---metal bonds, while an elevated coverage facilitates the latter case, in which the interaction between H_2O molecules weakens O–H bonding in H_2O and, thus, decreases bond dissociation energy.[27] In other words, a higher H_2O pressure contributes to the formation of larger hydrogen-bond networks and to the enhancement of water dissociation yields, which is consistent with our experimental data. We observe relatively higher yields of H_2O dissociation products (i.e., lower BE contributions) at elevated pressures in comparison with the higher BE component (i.e., peak IV) that is associated with molecularly adsorbed water, as shown in Fig. 2b. We have anticipated that coverage of the GaP surface with molecular water will be enhanced due to an increase in H_2O pressures, thereby greatly increasing the higher BE component of the O 1s spectra. However, as shown in Fig. 2b, the peak area of the lower BE components gradually increases with respect to the higher BE component at elevated pressures. Moreover, the maximum in the O1s spectra shifts toward lower BEs in Fig. 2b. This maximum moves from 532.7 eV (UHV and 0.005 mbar) to 532 eV (0.05 mbar) and then reaches 531.5 eV (0.5 mbar and 5 mbar). From such a dynamic change, we can deduce that, first, H_2O dissociates into O and OH; then, the formation of oxide adsorbates increases upon higher H_2O pressures.

Importantly, after H_2O is pumped away, the O 1s spectrum (Fig. 3b, top) indicates a significant increase of photoelectron signals corresponding to water dissociation products (peaks I, II and III). These signals are suppressed by that from molecularly adsorbed water during the *in situ* experiment. These spectra strongly support our conclusion regarding the enhancement of H_2O dissociation at higher pressures.

During the H_2O interaction with the surface atom M (where M = Ga or P), the OH adsorbate (M–OH) can have two configurations, bridging and atop,[4] due to the proton transfer process to the neighboring oxides (M–O–M), as shown schematically in Reaction (1):

M---OH_2 + M-O-M → M-OH (atop) + M-(OH)-M (bridging) (1)

The atop and bridge OH can be easily converted to oxides by losing one more H and releasing a gas-phase H_2 molecule to vacuum (Reaction 2):[57]

$$M\text{-}(OH)\text{-}M + M\text{-}H \rightarrow M\text{-}O\text{-}M + H_2 \tag{2}$$

Moreover, OH recombination reactions, in which OH adsorbates are converted to oxides assisted by water molecule desorption, can occur even at RT (Reaction 3):[61, 62]

$$M\text{-}OH + M\text{-}OH \rightarrow M\text{-}O\text{-}M + H_2O \tag{3}$$
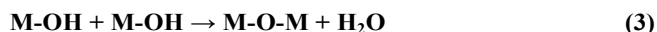
Admittedly, the water dissociation products can also recombine to produce gas-phase water (Reaction 4),[57] or local proton hopping can occur (Reaction 5):[4]

$$M\text{-}\text{-}\text{-}OH_2 + M \rightarrow M\text{-}OH + M\text{-}H \rightarrow M + M + H_2O \tag{4}$$

$$M\text{-}\text{-}\text{-}OH_2 + M\text{-}OH \rightarrow M\text{-}OH + M\text{-}\text{-}\text{-}OH_2 \tag{5}$$
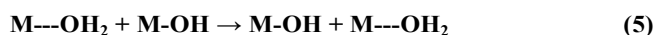
The formed oxides (M–O–M) in Reactions 2 and 3 can induce more water dissociation by accepting an H from a water molecule following Reaction 1.[4, 63] The oxygen-containing products of one reaction, hydroxyls and oxides, can be reactants of another dissociation reaction and thus promote further dissociation.[4, 63] Apart from a relatively high photoelectron intensity of molecularly adsorbed water in our *in situ* study as compared to earlier UHV studies,[14, 56] which showed that water molecules desorb at low temperatures (even below RT), we observe an even stronger signal intensity from the products of H_2O dissociation. The 6:1 peak area ratio between the adsorbed dissociation products and intact water molecules in the O 1s spectra after H_2O is pumped away indicates a high yield for water dissociation on the GaP(111) surface. The changes in the O 1s spectra clearly reflect the evolution of the water dissociation process in the Ga $2p_{3/2}$ spectra; a strong broadening effect at the higher BE side for both the Ga $2p_{3/2}$ (Fig. 2a) and the Ga 3d peak (Fig. S2b) at higher H_2O pressures indicates the oxidation and hydroxylation of surface Ga atoms. Because these changes in the Ga $2p_{3/2}$ spectra are more pronounced than those in the Ga 3d spectra, we conclude that the oxidation and hydroxylation mainly occur at the outmost atomic layers at RT, since the Ga 2p spectra are more surface-sensitive compared to the Ga 3d spectra.[44, 64, 65]

Simultaneously, a slightly broader and shifted P 2p peak at elevated pressures can suggest the formation of P–H bonds. Even though the XPS technique cannot pinpoint hydrogen-bond formation, an H adsorbate resulting from H_2O dissociation on the GaP surface is supported by calculations.[4, 6, 15, 16, 27, 66] It was estimated that the presence of P–H bonding can increase the water adsorption energy by 0.23-0.35 eV at a coverage of one monolayer.[4] A rigid interfacial water hydrogen-bond network promotes local proton hopping and thus enhances H_2O dissociation. As has been shown in computational modeling, the water dissociation products, OH and H, interact with Ga and P atoms, forming Ga–OH and P–H bonds, respectively.[27] Similarly, our study of H_2O interactions with the GaAs surface

exhibits peak broadening and shifts in the As ($2p_{3/2}$) spectra attributed to As–H bond formation at elevated pressures.[28] However, the IMFP of photoelectrons from the As 2p level (IMFP ~6.3 Å) is much shorter than that of the P 2p level (IMFP ~29 Å).[67] Therefore, the As 2p spectra are more surface sensitive than the P 2p spectra, while the P 2p spectra also contain a contribution from the lower-laying layers. This explains why the broadening effect in the P 2p spectra is not so clearly pronounced in the present study than that observed for GaAs.[28]

More dynamic chemistry is observed at elevated temperatures compared to that of the present pressure-dependent study. As mentioned above, in the temperature-dependent study, two distinctive regions are observed in which different chemistry occurs. From RT to 673 K, the hydroxylation and oxidation of Ga atoms and the hydration of P atoms occur, along with a possible desorption of H_2 (to be discussed later). Above 673 K, the oxidation of P atoms and the deeper-layer hydroxylation of Ga atoms occur by conversion of O–Ga–OH species via the intermediate Ga_2O-like species.

At temperatures below 673 K, fast oxidation and hydroxylation of Ga occur, as indicated by the largely broadened and shifted peaks toward higher BEs in the Ga $2p_{3/2}$ spectra, which are well-mirrored by changes in peak positions and shapes in the O 1s spectra. Upon heating, the interactions of H_2O with GaP are not restricted to the surface region, as demonstrated by the largely shifted Ga 3d spectra (Fig. S3b), which also include chemical information from deeper atomic layers. An increase in temperature facilitates H hopping at the H_2O/GaP interface and also leads to an enhanced yield of O–H bond breakage in adsorbed water molecules. As shown in Fig. 3a, the surface Ga atoms are largely hydroxylated and oxidized, with only a small contribution from Ga–P bonds at 673 K. Correspondingly, the lower BE portion of the O 1s spectra (Fig. 3b) exhibits two contributions that originate from intact water molecules (higher BE contribution, peak IV) and from products of water dissociation (lower BE contribution, peaks I, II, and III). The lower BE contribution exhibits a significant increase, indicating enhanced oxidation and hydroxylation of the GaP(111) surface. No significant changes are observed in the P 2p spectra below 673 K, with the exception of slightly less separated P $2p_{3/2}$ and P $2p_{2/1}$ peaks (Fig. 1e and S3c), which may suggest the formation of P–H. Because an H atom has an electronegativity higher than that of Ga, the attachment of H to a P atom would result in a shift of P 2p peaks toward higher BE and would overlap with P 2p peaks that originated from Ga–P bonds. Additionally, a strong quenching of P 2p signals is expected if the formation of dimer P–P and/or pure P–O phase occurs due to their high volatility.[68] Since the atomic ratio of Ga:P remains at 7:5 throughout the pressure-dependent experiment, it is assumed that Ga–P bonds are preserved. This constant ratio also suggests that stoichiometric Ga oxides, such as Ga_2O and Ga_2O_3, are unlikely to be formed under the present experimental conditions. Moreover, the production of Ga_2O and Ga_2O_3 would require oxygen diffusion into deeper layers of the

GaP crystal lattice and splitting of Ga–P bonds at a large scale, which is not observed in our photoelectron spectra. Therefore, a mixture of Ga oxides and hydroxides is expected to be formed at the H_2O/GaP interface, as represented by the structure of O_x–Ga–$(OH)_{3-x}$, which appear at a similar BE to that of stoichiometric Ga hydroxides (Ga–$(OH)_3$) reported in previous UHV studies.[41-44]

Upon heating above 673 K, oxidation of P atoms is observed, which is evident from the peak appearance at a BE of ~ 134 eV in the P 2p spectra (Figs. 1e and S4). However, we believe that most of the P atoms are still bonded to Ga atoms within a crystal lattice rather than bonded to P or O atoms. As obtained from computational modeling, the Ga–O–Ga structure is more stable, by approximately 0.5 eV, than the Ga–O–P structure.[6, 15] Therefore, P oxidation is a kinetically controlled process at high temperatures at which large-scale oxidation is initiated as a result of more reactive species generated on the surface region. It is unlikely that the formation of P_2O_5 occurs in the pure phase, for which the BE was reported between 134-136 eV.[42-44, 58] Instead, these oxides are most likely to be in the form of O=P(Ga)–O–Ga than in the form of pure-phased P oxides that are highly volatile.[68] A certain kind of Ga and P oxide/hydroxide network with the schematic formula of $Ga_aP_bO_c(OH)_d$ (a, b, c, and d represent a ratio of different elements and groups) may be formed at the H_2O/GaP interface. Such a $Ga_aP_bO_c(OH)_d$ network-like structure may eventually help to stabilize the newly formed P oxides/hydroxides. The possible mechanisms of chemical processes at elevated pressures and temperatures are presented in Fig. 5, with a suggested configuration of the chemical environment of P atoms.
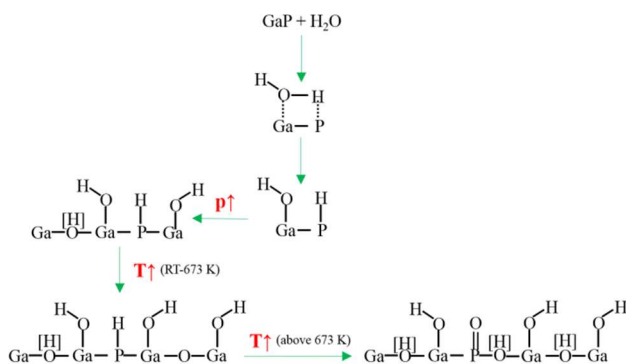
Fig. 5 Possible mechanisms of water dissociation onto the GaP(111) surface under elevated pressures and temperatures. Note: an H atom can easily diffuse on the surface; therefore, [H] represents the formation of Ga-O-Ga or Ga-O(H)-Ga bridges.

Interestingly, the dynamic conversion of surface species that were previously formed at elevated pressures in the lower temperature region into large-scale Ga hydroxides, along with the oxidation of surface P atoms, is observed above 673 K and was not predicted by previous calculations. A relatively high temperature (≥773 K) provides sufficient energy to overcome certain activation barriers and eventually facilitates

transformation of O–Ga–OH and Ga oxides to Ga hydroxides accompanied by P oxidation. The evolution of Ga $2p_{3/2}$ spectra (Fig. 3a) indicates a signal decrease for O–Ga–OH species along with a signal increase for Ga_2O-like and O_x–Ga–$(OH)_{3-x}$ species. This suggests that O–Ga–OH acts as a precursor for other species formed at temperatures above 673 K. After O–Ga–OH species are mainly converted into Ga_2O-like species at the boundary of two temperature regions, the newly formed Ga_2O-like species are relatively unstable and are converted to O_x–Ga–$(OH)_{3-x}$, which is particularly clearly seen at the elevated pressure of 0.5 mbar (Fig. 3). Moreover, the peak area ratios of O_x–Ga–$(OH)_{3-x}$ and Ga_2O-like species change within four hours of exposure to an H_2O pressure of 0.1 mbar and at 773 K, as displayed in Fig. 4. Such a time-dependent study indicates that prolonged heating at a fixed pressure and temperature causes vigorous changes in the surface chemistry until an equilibrium is reached.

Finally, it is predicted by several calculations that gas-phase molecular hydrogen can be released from the H_2O/GaP interface (e.g., Reaction 2).[4, 6, 15] However, H_2 is not observed in the present study within the experimental design and detection limit. There is a possibility that H_2 abundance is insufficient to be detected by a mass spectrometer (MS) attached to the chamber, which is separated from the reaction cell by another chamber coupled to the differentially pumped system of the HEA.[28] Similarly, no H_2 detection was reported in our previous study on H_2O dissociative adsorption onto the GaAs(100) surface.[28] On the other hand, the large-scale formation of Ga hydroxides or $Ga_aP_bO_c(OH)_d$ networks could prevent H_2 formation. As suggested by Wood et al., a rigid structure of the hydrogen-bond network is formed at the H_2O/GaP interface, and long-range proton hopping is kinetically limited.[4] Consequently, such a confined region, where H_2O dissociation is initiated and H_2 is formed, becomes a catalytic site for water splitting or a nucleation site for photo-corrosion reactions.

Conclusions

We monitored the chemical evolution of H_2O dissociation on the GaP(111) surface using NAP XPS. Our results suggest that H_2O dissociative adsorption and the subsequent hydroxylation and oxidation of the surface Ga and P atoms occur at large scales at elevated H_2O pressures and temperatures. This observation is in good agreement with theoretical calculations of H_2O interaction with the GaP surface, which showed that at higher H_2O coverage Ga (and P), hydroxylation and oxidation are greatly amplified due to the formation of hydrogen-bond networks with stronger intermolecular interactions that lower the water dissociation barrier.[4, 6, 15, 27, 59] The formation of Ga hydroxide species and P oxides at elevated temperatures facilitates the formation of $Ga_aP_bO_c(OH)_d$ network-like structures comprising preserved Ga–P bonds in addition to the formation of O-based compounds involving both elements.

Furthermore, such a highly oxidized GaP surface can provide evidence for the photo-corrosion process of GaP-based PEC solar cells. As reported earlier, an M-O-M (where M represents Ga or P) bridge can create a trap for hole carriers due to the lattice strain or chemical environment of the M atoms,

and such a trapped hole may contribute to the observed photo-corrosion of GaP/InP-based electrodes in PEC cells.[4, 15, 24, 69-73] Therefore, our research can greatly contribute to establishing an atomistic understanding of the generation and roles of surface oxygen species to improve the designs of PEC devices that can resist or reduce corrosion processes while maintaining efficient electron transfer. Since proton transfer can passivate surface dangling bonds and "self-protect" the material surface,[4] limited proton transfer could be another process that leads to photo-corrosion of GaP-based electrodes. Currently, a cell with a monolithic GaInP$_2$/GaAs absorber results in a 12.4% solar-to-hydrogen efficiency, which is the highest efficiency achieved for PEC water splitting.[5, 74, 75] The use of GaP in earlier PEC devices showed limitations such as corrosion and low efficiency for electron extraction due to the formation of an oxide layer.[5, 75] The formation of oxide layers is consistent with our present study. However, functionalized InP can overcome these limitations through the formation of a mixture of oxides and phosphates on the surface that are thermodynamically stable and exhibit good dielectric properties.[5, 53, 76] Therefore, it would be interesting to determine the role of Ga and In in a GaInP$_2$-based PEC device in terms of their chemical behavior at the H$_2$O/semiconductor interface. A further study will be performed in our laboratory to understand H$_2$O interactions with such modified surfaces at the atomic level.

Acknowledgements

Notes and references

^{a} Radiation Laboratory, University of Notre Dame, Notre Dame, IN 46556, USA

^{b} Department of Chemistry and Biochemistry, University of Notre Dame, Notre Dame, IN 46556, USA

^{c} Department of Physics, University of Notre Dame, Notre Dame, IN 46556, USA

Electronic Supplementary Information (ESI) available: [Evolutions of spectra obtained from pressure-, temperature- and time-dependent studies]. See DOI: 10.1039/b000000x/

1. Lewis, N. S.; Nocera, D. G. *P. Natl. Acad. Sci. USA* 2006, **103**, 15729.
2. Fujishima, A.; Honda, K. *Nature* 1972, **238**, 37.
3. Tomkiewicz, M.; Woodall, J. M. *Science* 1977, 196, 990.
4. Wood, B. C.; Schwegler, E.; Choi, W. I.; Ogitsu, T. *J. Am. Chem. Soc.* 2013, **135**, 15774.
5. Lewerenz, H.-J., L.; Peter, L., *Photoelectrochemical Water Splitting: Materials, Processes and Architectures*; Royal Society of Chemistry: Cambridge, GBR, 2013.
6. Jeon, S.; Kim, H.; Goddard, W. A.; Atwater, H. A. *J. Phys. Chem. C* 2012, **116**, 17604.
7. Walter, M. G.; Warren, E. L.; McKone, J. R.; Boettcher, S. W.; Mi, Q. X.; Santori, E. A.; Lewis, N. S. *Chem. Rev.* 2010, **110**, 6446.
8. Sun, J. W.; Liu, C.; Yang, P. D. *J. Am. Chem. Soc.* 2011, 133, 19306.
9. Khaselev, O.; Turner, J. A. *Science* 1998, **280**, 425.
10. Paracchino, A.; Laporte, V.; Sivula, K.; Gratzel, M.; Thimsen, E. *Nat. Mater.* 2011, **10**, 456.
11. Cherry, R. S. *Int. J. Hydrogen Energ.* 2004, **29**, 125.
12. Brouwer, *Curr. Appl. Phys.* 2010, **10**, S9.
13. Akimov, A. V.; Muckerman, J. T.; Prezhdo, O. V. *J. Am. Chem. Soc.* 2013, **135**, 8682.
14. May, M. M.; Supplie, O.; Hohn, C.; van de Krol, R.; Lewerenz, H. J.; Hannappel, T. *New J. Phys.* 2013, **15**, 103003.
15. Wood, B. C.; Ogitsu, T.; Schwegler, E. *J. Chem. Phys.* 2012, **136**, 064705.
16. Wood, B. C.; Ogitsu, T.; Schwegler, E. *J. Photon. Energy.* 2011, **1**, 016002.
17. Sato, S.; Arai, T.; Morikawa, T.; Uemura, K.; Suzuki, T. M.; Tanaka, H.; Kajino, T. *J. Am. Chem. Soc.* 2011, **133**, 15240.
18. Kim, Y. H.; Jun, Y. W.; Jun, B. H.; Lee, S. M.; Cheon, J. W. *J. Am. Chem. Soc.* 2002, **124**, 13656.
19. Chitambar, M.; Wang, Z. J.; Liu, Y. M.; Rockett, A.; Maldonado, S. *J. Am. Chem. Soc.* 2012, **134**, 10670.
20. del Alamo, J. A. *Nature* 2011, **479**, 317.
21. Hu, S.; Shaner, M. R.; Beardslee, J. A.; Lichterman, M.; Brunschwig, B. S.; Lewis, N. S. *Science* 2014, **344**, 1005.
22. Wallentin, J.; Anttu, N.; Asoli, D.; Huffman, M.; Aberg, I.; Magnusson, M. H.; Siefer, G.; Fuss-Kailuweit, P.; Dimroth, F.; Witzigmann, B.; Xu, H. Q.; Samuelson, L.; Deppert, K.; Borgstrom, M. T. *Science* 2013, **339**, 1057.
23. Kobayashi, Y.; Kumakura, K.; Akasaka, T.; Makimoto, T. *Nature* 2012, **484**, 223.
24. Khaselev, O.; Turner, J. A. *J. Electrochem. Soc.* 1998, **145**, 3335.
25. Massies, J.; Contour, J. P. *Appl. Phys. Lett.* 1985, **46**, 1150.
26. Williams, K. S.; Lenhart, J. L.; Andzelm, J. W.; Bandara, S. V.; Baril, N. F.; Henry, N. C.; Tidrow, M. Z. *Surf. Sci.* 2014, **622**, 71.
27. Munoz-Garcia, A. B.; Carter, E. A. *J. Am. Chem. Soc.* 2012, **134**, 13600.
28. Zhang, X. Q.; Ptasinska, S. *J. Phys. Chem. C* 2014, 118, 4259.
29. Montgomery, V.; Williams, R. H. *J. Phys. C. Solid State* 1982, **15**, 5887.
30. Henrion, O.; Klein, A.; Jaegermann, W. *Surf. Sci.* 2000, **457**, L337.
31. Zhang, X.; Lamere, E.; Liu, X., Y.; Furdyna, J. K.; Ptasinska, S. *Chem. Phys. Lett.* 2014, **605-606**, 51.
32. Bermudez, V. M. *J. Appl. Phys.* 2013, **113**, 184906.
33. Salmeron, M.; Schlogl, R. *Surf. Sci. Rep.* 2008, 63, 169.
34. Starr, D. E.; Liu, Z.; Havecker, M.; Knop-Gericke, A.; Bluhm, H. *Chem. Soc. Rev.* 2013, **42**, 5833.
35. Mazin, B. A.; Sank, D.; McHugh, S.; Lucero, E. A.; Merrill, A.; Gao, J. S.; Pappas, D.; Moore, D.; Zmuidzinas, J. *Appl. Phys. Lett.* 2010, **96**, 102504.
36. Iwasaki, H.; Mizokawa, Y.; Nishitani, R.; Nakamura, S. *Surf. Sci.* 1979, **86**, 811.
37. Mizokawa, Y.; Komoda, O.; Iwasaki, H.; Shen, D. H.; Nakamura, S. *J. Electron. Spectrosc.* 1983, **31**, 335.
38. Naitoh, M.; Konishi, A.; Inenaga, H.; Nishigaki, S.; Oishi, N.; Shoji, F. *Surf. Sci.* 1998, **402**, 623.

39. Naitoh, M.; Watanabe, A.; Konishi, A.; Nishigaki, S. *Jpn. J. Appl. Phys. 1* 1996, **35**, 4789.

40. Oishi, N.; Shoji, F.; Konishi, A.; Naitoh, M.; Nishigaki, S. *Surf. Rev. Lett.* 1998, **5**, 223.

41. Priyantha, W.; Radhakrishnan, G.; Droopad, R.; Passlack, M. *J. Cryst. Growth* 2011, **323**, 103.

42. Epp June; Dillard, J. G. *Chem. Mater.* 1989, **1**, 325.

43. McDonnell, S.; Dong, H.; Hawkins, J. M.; Brennan, B.; Milojevic, M.; Aguirre-Tostado, F. S.; Zhernokletov, D. M.; Hinkle, C. L.; Kim, J.; Wallace, R. M. *Appl. Phys. Lett.* 2012, **100**, 141606.

44. Hinkle, C. L.; Vogel, E. M.; Ye, P. D.; Wallace, R. M. *Curr. Opin. Solid St. M.* 2011, **15**, 188.

45. Andersson, K.; Ketteler, G.; Bluhm, H.; Yamamoto, S.; Ogasawara, H.; Pettersson, L. G. M.; Salmeron, M.; Nilsson, A. *J. Am. Chem. Soc.* 2008, **130**, 2793.

46. Andersson, K.; Ketteler, G.; Bluhm, H.; Yamamoto, S.; Ogasawara, H.; Pettersson, L. G. M.; Salmeron, M.; Nilsson, A. *J. Phys. Chem. C* 2007, **111**, 14493.

47. Arrigo, R.; Havecker, M.; Schuster, M. E.; Ranjan, C.; Stotz, E.; Knop-Gericke, A.; Schlogl, R. *Angew. Chem. Int. Edit.* 2013, **52**, 11660.

48. Casalongue, H. S.; Kaya, S.; Viswanathan, V.; Miller, D. J.; Friebel, D.; Hansen, H. A.; Norskov, J. K.; Nilsson, A.; Ogasawara, H. *Nat. Commun.* 2013, **4**, 2817.

49. Hinkle, C. L.; Milojevic, M.; Brennan, B.; Sonnet, A. M.; Aguirre-Tostado, F. S.; Hughes, G. J.; Vogel, E. M.; Wallace, R. M. *Appl. Phys. Lett.* 2009, **94**, 162101.

50. Zhang, X.; Lamere, E.; Liu, X.; Furdyna, J. K.; Ptasinska, S. *Appl. Phys. Lett.* 2014, **104**, 181602.

51. Chen, G.; Visbeck, S. B.; Law, D. C.; Hicks, R. F. *J. Appl. Phys.* 2002, **91**, 9362.

52. Shibata, N.; Ikoma, H. *Jpn. J. Appl. Phys. 1* 1992, **31**, 3976.

53. Adelmann, C.; Cuypers, D.; Tallarida, M.; Rodriguez, L. N. J.; De Clercq, A.; Friedrich, D.; Conard, T.; Delabie, A.; Seo, J. W.; Locquet, J. P.; De Gendt, S.; Schmeisser, D.; Van Elshocht, S.; Caymax, M. *Chem. Mater.* 2013, **25**, 1078.

54. Gresch, R.; Mullerwarmuth, W.; Dutz, H. *J. Non-Cryst. Solids* 1979, **34**, 127.

55. Guivarch, A.; Lharidon, H.; Pelous, G.; Hollinger, G.; Pertosa, P. *J. Appl. Phys.* 1984, **55**, 1139.

56. Chung, C. H.; Yi, S. I.; Weinberg, W. H. *J. Vac. Sci. Technol. A* 1998, **16**, 1785.

57. Henderson, M. A. *Surf. Sci. Rep.* 2002, **46**, 1.

58. Schmeisser, D.; Himpsel, F. J.; Hollinger, G.; Reihl, B. *Phys. Rev. B* 1983, **27**, 3279.

59. Donadio, D.; Ghiringhelli, L. M.; Delle Site, L. *J. Am. Chem. Soc.* 2012, **134**, 19217.

60. Tatarkhanov, M.; Ogletree, D. F.; Rose, F.; Mitsui, T.; Fomin, E.; Maier, S.; Rose, M.; Cerda, J. I.; Salmeron, M. *J. Am. Chem. Soc.* 2009, **131**, 18425.

61. Yamamoto, S.; Bluhm, H.; Andersson, K.; Ketteler, G.; Ogasawara, H.; Salmeron, M.; Nilsson, A. *J. Phys-Condens. Mat.* 2008, **20**, 184025.

62. Bange, K.; Grider, D. E.; Madey, T. E.; Sass, J. K. *Surf. Sci.* 1984, **137**, 38.

63. Wood, B. C.; Schwegler, E.; Choi, W. I.; Ogitsu, T. *J. Phys. Chem. C* 2014, **118**, 1062.

64. Surdu-Bob, C. C.; Saied, S. O.; Sullivan, J. L. *Appl. Surf. Sci.* 2001, **183**, 126.

65. Hinkle, C. L.; Milojevic, M.; Vogel, E. M.; Wallace, R. M. *Appl. Phys. Lett.* 2009, **95**, 151905.

66. Wood, B. C.; Ogitsu, T.; Schwegler, E. In *Ab Initio Modeling of Water-Semiconductor Interfaces for Direct Solar-to-Chemical Energy Conversion*, Solar Hydrogen and Nanotechnology V, San Diego, California, 2010, SPIE: 7770.

67. Powell, C. J.; Jablonski, A., *Nist Standard Reference Database 71: Nist Electron Inelastic Mean Free Path Database: Version 1.2*; National Institute of Standards and Technology: Gaithersburg, Maryland, USA, 2010.

68. Norman, N. G., *Chemistry of the Elements; 2nd Ed.*; Butter worth-Heinemann: Earnshaw, Alan, 1997.

69. Vigneron, J.; Herlem, A.; Khoumri, E. M.; Etcheberry, A. *Appl. Surf. Sci.* 2002, **201**, 51.

70. Lewerenz, H. J.; Aspnes, D. E.; Miller, B.; Malm, D. L.; Heller, A. *J. Am. Chem. Soc.* 1982, **104**, 3325.

71. Spicer, W. E.; Lindau, I.; Skeath, P.; Su, C. Y.; Chye, P. *Phys. Rev. Lett.* 1980, **44**, 420.

72. Heller, A.; Miller, B.; Lewerenz, H. J.; Bachmann, K. J. *J. Am. Chem. Soc.* 1980, **102**, 6555.

73. Heller, A. *Science* 1984, **223**, 1141.

74. Schulte, K. H.; Lewerenz, H. J. *Electrochim. Acta.* 2002, **47**, 2633.

75. Lewerenz, H. J.; Heine, C.; Skorupska, K.; Szabo, N.; Hannappel, T.; Vo-Dinh, T.; Campbell, S. A.; Klemm, H. W.; Munoz, A. G. *Energ. Environ. Sci.* 2010, **3**, 748.

76. Robach, Y.; Besland, M. P.; Joseph, J.; Hollinger, G.; Viktorovitch, P.; Ferret, P.; Pitaval, M.; Falcou, A.; Post, G. *J. Appl. Phys.* 1992, **71**, 2981.

Physical Chemistry Chemical Physics Accepted Manuscript
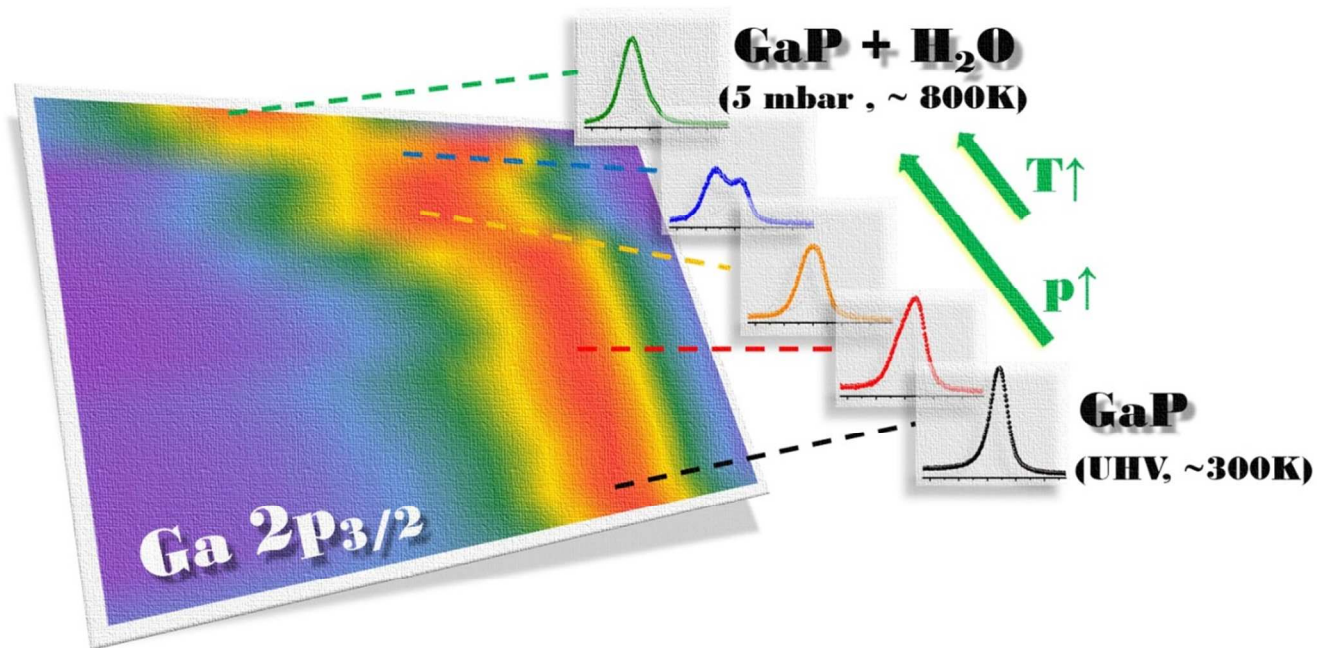
Graphical abstract: Chemical evolution bridging UHV and near-realistic conditions at the H₂O/GaP interface.